Feasible delivery system based on poly(lactictide-co-glycolide) nanoparticles loaded with antimicrobial mupirocin for possible wound healing

Ludmila Košarišťanová[1], Tomáš Komprda[2], Vendula Popelková[2], Tatiana Fialová[1], Pavla Vymazalová[2], Carlos E. Astete[3]

[1]Mendel University in Brno, Faculty of AgriSciences, Department of Chemistry and Biochemistry, Brno, Czech Republic
[2] Mendel University in Brno, Faculty of AgriSciences, Department of Food Technology, Brno, Czech Republic
[3] Louisiana State University, College of Engineering, Department of Biological and Agricultural Engineering, Baton Rouge, Louisiana, USA

Received January 9, 2023
Accepted July 11, 2023

Abstract

The objective of the study was to assess cytotoxicity (based on the dimethylthiazol–diphenyltetrazolium bromide cell viability assay) and antimicrobial effects of poly(lactictide-co-glycolide) nanoparticles with entrapped mupirocin (PLGA/MUP NPs) on *Staphylococcus aureus* and methicillin-resistant *S. aureus* (MRSA) strains using a disk-diffusion method, cryo-scanning electron microscopy (cryo-SEM) and fluorescence microscopy. Based on the evaluation of the growth curve, PLGA/MUP NPs inhibited growth of the both tested strains already at a concentration of 0.29 μg/ml, and their inhibitory effect at concentrations from 0.29 to 1.17 μg/ml was comparable with free MUP using the disk-diffusion method. PLGA/MUP NPs also tended to increase the abundance of the dead cells of MRSA, but not of *S. aureus*, in comparison with free MUP when evaluated by fluorescence microscopy. Further, cryo-SEM evaluation demonstrated an antibacterial-inhibitory effect of PLGA/MUP NPs on *S. aureus* in a dose-dependent manner. On the other hand, PLGA/MUP NPs cytotoxic activity tended to be substantially lower in comparison with both free MUP and empty PLGA NPs. It can be concluded that the excellent biocompatibility and satisfactory antibacterial effects of PLGA/MUP NPs constitute a suitable alternative as far as cutaneous wound healing is concerned.

Cytotoxicity, Staphylococcus aureus, cryo-scanning electron microscopy, fluorescence microscopy, disk-diffusion test

Studies on improving the healing process of acute and chronic wounds have sought to develop innovative and effective wound dressing materials with incorporated drugs that could accelerate healing or to prevent frequently occurring complicating factors (Rajendran et al. 2018). The aim of many studies is to deliver drugs directly to the site of action, thereby increasing their efficacy (Smith et al. 2020), a goal which can be achieved with targeting nanodelivery systems. Nanoparticle (NP) drug delivery systems are considered promising solutions for topical delivery of antibacterial agents to fight resistant microorganisms and subsequently overcome microbial resistance (Ma and Mumper 2013). These systems also offer protection against degradation and enable a controlled release of the drug (Tang et al. 2021). Several types of NPs were developed for wound healing (Berthet et al. 2017), including those based on natural polymers (e.g. chitosan; Lin et al. 2017) or synthetic polymers, including poly(lactic-co-glycolic) acid (PLGA) (Chereddy et al. 2014; Hasan et al. 2019; Basaran et al. 2021).

The antibacterial properties of NPs have already been established (Hajipour et al. 2012). Antibiotic-loaded polymeric nanoparticles were successfully tested, among others, in the case of methicilin-resistant *Staphylococcus aureus* (MRSA) infection: PLGA NPs with entrapped clindamycin accelerated healing in a mouse model of MRSA-infected cutaneous wounds (Hasan et al. 2019). Enhanced anti-inflammatory and antibacterial activity

Address for correspondence:
Tomas Komprda
Department of Food Technology
Mendel University in Brno
Zemedelska 1, 613 00 Brno, Czech Republic

Phone: +420 545 133 261
E-mail: komprda@mendelu.cz
http://actavet.vfu.cz/

of levofloxacin nano-delivered by PLGA NPs was also demonstrated in a model of *S. aureus* keratitis (Cheng et al. 2021).

One of the drugs that can be loaded into NPs is the antibiotic mupirocin (MUP) (Alcantara et al. 2019). Mupirocin is a topical antibiotic primarily effective against gram-positive staphylococci and streptococci (Sundaramoorthy et al. 2021). It has proven effective for treatment of invasive *Staphylococcus aureus* infections (Goldmann et al. 2019). Mupirocin blocks RNA and protein synthesis in bacteria, but it is not associated with significant human toxicity (Khoshnood et al. 2019).

The objective of the present study was to test cytotoxicity and antimicrobial activities of the MUP-loaded PLGA NPs against *S. aureus*, including MRSA, with the intention to assess their suitability for treatment of cutaneous wounds, including development of an alternative antimicrobial therapy or enhancing the MUP efficacy amidst increasing incidence of MUP resistance in MRSA clinical isolates (Perumal et al. 2022).

Materials and Methods

Synthesis of NPs

The following chemicals were used in the NPs' preparation: dichloromethane (DCM, anhydrous: 99.8%; Sigma-Aldrich, St. Louis, MO, USA); poly(lactic-co-glycolic) acid (PLGA; MW 38,000–54,000 g/mol; lactide:glycolide ratio of 50:50; Sigma-Aldrich); hexane (95%; JT Baker Chemical Co., Phillipsburg, NJ); polyvinyl alcohol (PVA, 98–99%, hydrolyzed, MW 31,000–50,000 g/mol; Sigma-Aldrich); trehalose dihydrate (99.0%, MW 378,33 g/mol; Sigma-Aldrich); nanopure water (Nanopure Diamond; USA); 0.2 µm Barnsted D3750 Hollow Fiber Filter (Barnsted International, Dubuque, IA, USA); mupirocin (MUP; Sigma-Aldrich); ethyl acetate (EMD Chemicals Inc., Gibbstown, NJ, USA).

Nanoparticles were synthesized by the emulsion evaporation method (Astete and Sabliov 2006). The organic phase contained 220 mg of PLGA, 5 ml of ethyl acetate and 11 mg of MUP. The aqueous phase was comprised of 2% PVA. The organic phase was added to the aqueous phase drop-wise under stirring at 220 rpm and the formed emulsion was microfluidized four times at 30,000 psi using a microfluidizer M 110P (Microfluidics, MA, USA). The solvent was then evaporated under vacuum using a rotoevaporator (R-124, Rotovap, Buchi Inc., New Castle, DE, USA) for 60 min (40 mm Hg; stirring at 60 rpm). Nanoparticles were then dialyzed for two days (25 °C) to remove excess PVA using 300 kDa Spectra/POR CE membrane (Spectrum Rancho, CA, USA). Subsequently, the samples were mixed (1:1, w/w) with 650 mg of trehalose, frozen for 30 min in freezer and then freeze-dried for two days (2.5-plus freezone; Labconco Corporation, MO, USA). The NP powder was stored in dark refrigerated conditions (under –20 °C) until further analysis. Control NPs free of MUP (PLGA NPs) were prepared by the same procedure as mentioned above, only without MUP.

As far as the morphology of the loaded and empty PLGA NPs is concerned, the mean size was 141.1 and 190.7 nm, polydispersity index (indicating the size distribution) had the value of 0.336 and 0.218, and ζ-potential was –21.9 and –4.95 mV, respectively. The loading capacity and the entrapment efficiency of MUP was 2.34 µg MUP/mg powder and 22.4%, respectively. Regarding the MUP release profile, more than 80% of MUP was released in 24 h and 100% was released in 48 h (Vymazalova et al. 2020; Komprda et al. 2022a).

Microbiological evaluation

For microbiological evaluation, the tested samples of PLGA NPs (empty) and PLGA-MUP NPs were dissolved in MilliQ water and sonicated for 5 min (40 kHz).

Cultivation of the tested bacterial strains

Staphylococcus aureus (CCM 4223) and MRSA (CCM 7110) were obtained from the Czech Collection of Microorganisms (Masaryk University, Brno, Czech Republic). The bacterial strains were cultured on 5% Columbia blood agar (LMS, Czech Republic) at 37 °C overnight.

The disk diffusion method based on the European Committee on Antimicrobial Susceptibility Testing (EUCAST) manual and evaluation of the growth curve of the bacterial strains (*S. aureus*; MRSA) are described in our previous publication (Komprda et al. 2022a).

Fluorescence microscopy

Samples of MUP and PLGA-MUP-PVA NPs, respectively, with MUP concentrations of 0.585 and 1.17 µg/ml, were used for the testing of their antibacterial effect on *S. aureus* and MRSA. The samples were incubated in a rotator together with a bacterial culture with the optical density of 10^8 CFU/ml in TSB (Trypton soy broth, Oxoid) at 37 °C overnight. As a control, bacterial culture alone in TSB medium was used. After incubation, bacterial cells were purified by centrifugation and the TSB was replaced with PBS. To stain the bacteria, LIVE/DEAD BacLight Bacterial Viability and Counting Kit (Thermo Fisher Scientific, Waltham, USA) was

used according to manufacturer's instructions. After incubation, the samples were observed by OLYMPUS IX71 (Olympus, Tokyo, Japan) inverted fluorescence microscope at × 200 magnification.

Cryo-scanning electron microscopy (cryo-SEM)

The graphite electrodes were washed with 70% isopropyl alcohol, dried, and irradiated by UV light for 5 min. Bacterial culture of *S. aureus* was diluted in Mueller Hinton Broth to 0.5 McFarland. The graphite electrodes were placed in a 24-well plate, embedded in bacterial culture and incubated at 37 °C for 4 h. After incubation, the broth with bacterial culture was removed and MUP/PLGA NPs were added at different concentrations (0.59–1.17 μg of MUP/ml). The graphite electrodes with samples were incubated at 37 °C for 24 h. After incubation, the NPs were removed and graphite electrodes were rinsed gently with 2 ml of PBS three times. After rinsing, the graphite electrodes were dried for 30 min. CRYO system PP3010 from Quorum Technologies (Quorum Technologies Ltd, Sussex, UK) was used. *Staphylococcus aureus* on carbon stub was transferred to the copper holder and frozen in liquid nitrogen. The samples were transferred under vacuum conditions to the SEM chamber equipped with a cryo-stage and observed under high vacuum conditions. The samples were examined by SEM Tescan MAIA 3 equipped with a field emission gun (FEG; Tescan Ltd., Brno, Czech Republic). The best pictures were obtained using the In-lens SE detector at working distance between 2.79–3.02 mm and at 1 kV acceleration voltage. Pixel images 768 × 858 were obtained at × 4.400–8.620 magnification covering a sample area of 4.68−24.10 μm. Full frame capture was performed in a Depth mode. Accumulation of image with image shift correction was carried on within approximately 0.5 min with the ~1 μs/pixel dwell time. Spot size was set at 8.5 nm.

Cytotoxicity testing

Cell viability was assessed using the MTT assay with spontaneously transformed aneuploid immortal keratinocyte cell line from adult human skin (HaCaT) as described in our previous paper (Komprda et al. 2022a).

Statistical evaluation

Differences between the tested samples were statistically evaluated by paired *t*-test using the Statistica 12 package (StatSoft, Tulsa, OK, USA). A P value < 0.05 was considered significant.

Results

Bacterial inhibition determined by the growth curve method

Growth of *S. aureus* and MRSA was monitored by optical density within 21 h. Empty PLGA NPs did not affect the growth of the tested bacterial strains at all (data not shown). In contrast, PLGA/MUP NPs inhibited growth of *S. aureus* and MRSA at all tested concentrations (1.17 μg/ml, 0.585 μg/ml, 0.293 μg/ml; Fig. 1), similarly to free MUP (data not shown). The inhibition effect of PLGA/MUP NPs at the concentration of 1.17 μg/ml was 96.6% for *S. aureus* and 84.4% for MRSA. However, the MRSA strain began to grow again after 16 h of treatment (Fig. 1B). The MUP concentration of 0.585 μg/ml and 0.293 μg/ml in PLGA/MUP NPs reduced growth of *S. aureus* by 58% and 44%, respectively. The MRSA strain was inhibited by 48% at concentration of 0.585 μg/ml and by 29% at concentration of 0.293 μg/ml.

Inhibition activity evaluated by the disk diffusion method

In accordance with the results concerning the growth curve, empty PLGA NPs did not show an antimicrobial effect against the tested bacterial strains (data not shown), but both *S. aureus* and MRSA showed sensitivity to PLGA/MUP NPs. From the extent of the inhibition zone surrounding the disk (Plate XIII, Fig. 2A), it is apparent that the inhibition by PLGA/MUP NPs is comparable to free MUP, except for the highest concentration of 2.34 μg/ml (Fig. 2B), where a higher ($P < 0.05$) inhibitory activity of free MUP was established. The inhibitory activity of nano-delivered MUP did not differ significantly ($P > 0.05$) from free MUP at concentrations ranging from 0.585 to 1.17 μg/ml.

The antibacterial effect assessed by fluorescence microscopy

The live/dead assay combined with fluorescence microscopy was utilized for the visualization of living and dead bacterial cells using fluorescent dyes SYTO9 and propidium iodide. The fluorescence images of *S. aureus* and MRSA treated with PLGA/MUP NPs and

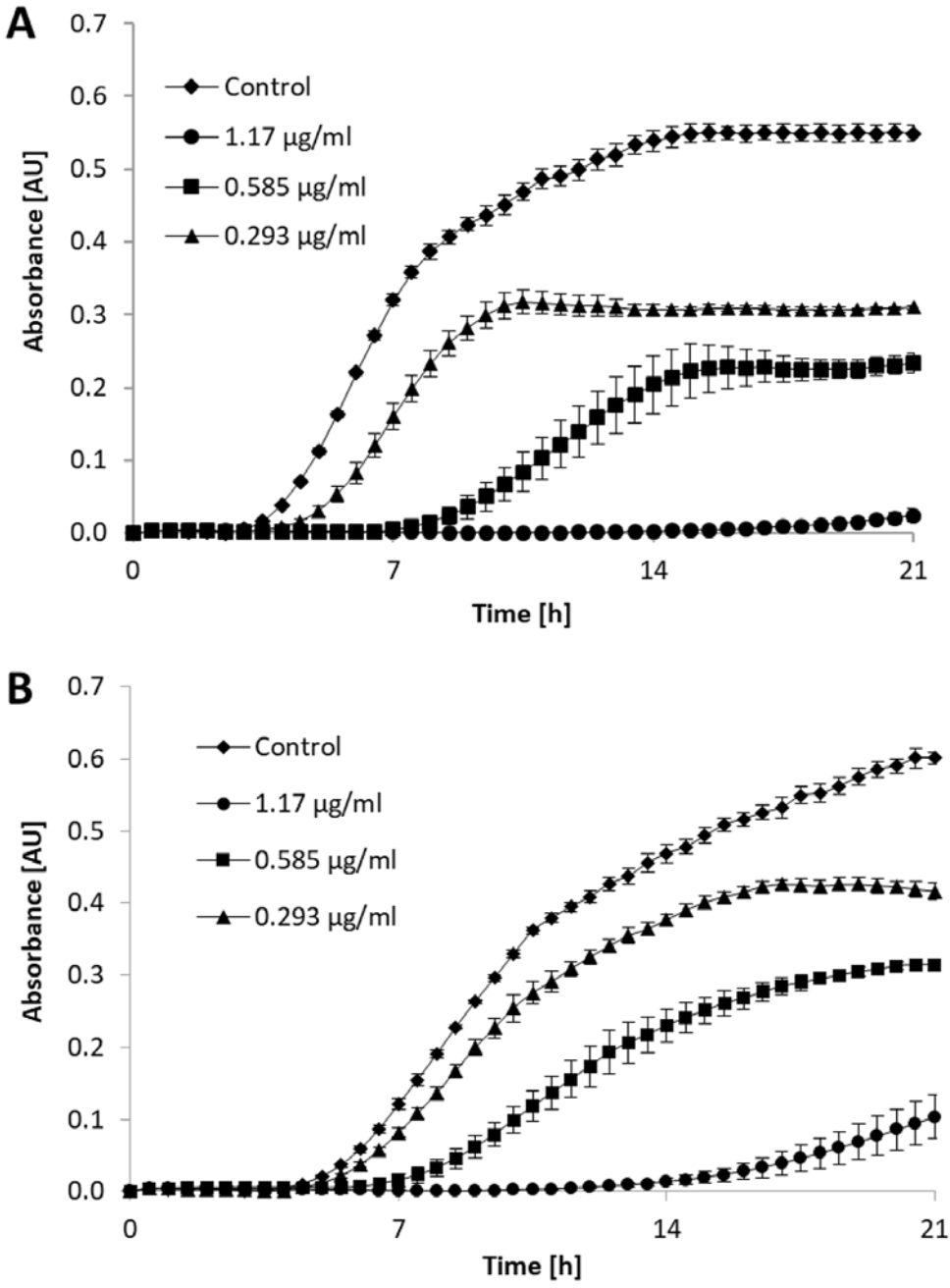

Fig. 1. Growth curves of *Staphylococcus aureus* (A) and methicillin-resistant *S. aureus* (MRSA; B) treated with different concentrations of poly(lactictide-co-glycolide) nanoparticles loaded with mupirocin (control: non-treated bacterial culture)

MUP alone are shown in Fig. 3 (Plate XIII). Both encapsulated and free MUP caused the reduction of all (live + dead) cells of the both tested strains (green spots) compared to control (bacterial culture alone in TSB medium).

The presence of higher amount of red spots indicates the loss of bacterial membrane integrity due to membrane damage causing cell death: the encapsulated MUP at both concentrations noticeably increased the abundance of dead cells (red spots) of the both bacterial strains. For free MUP, this phenomenon is observable only at the concentration of 0.585 μg/ml in the case of *S. aureus*.

The morphology of the PLGA/MUP-treated strains observed by cryo-SEM

The surface of treated (PLGA/MUP NPs) and untreated (control) *S. aureus* and MRSA cells is shown in Fig. 4. In comparison with control, increasing concentration of the nano-encapsulated MUP tended to decrease numbers of cells of *S. aureus* in a dose-dependent manner (the trend is better observable at the higher magnification: the right columns in Fig. 4. Thus, a more conspicuous inhibitory effect of encapsulated MUP on *S. aureus* was found at the concentration of 1.17 μg/ml. However, as far as MRSA is concerned, no clear concentration-dependent effect of PLGA/MUP NPs on the number of cells was observed. Rather, though encapsulated MUP at the concentration of 0.585 μg/ml tended to decrease MRSA cells compared to control, the MRSA numbers tended to increase again after treatment with PLGA/MUP at the higher concentration (1.17 μg/ml).

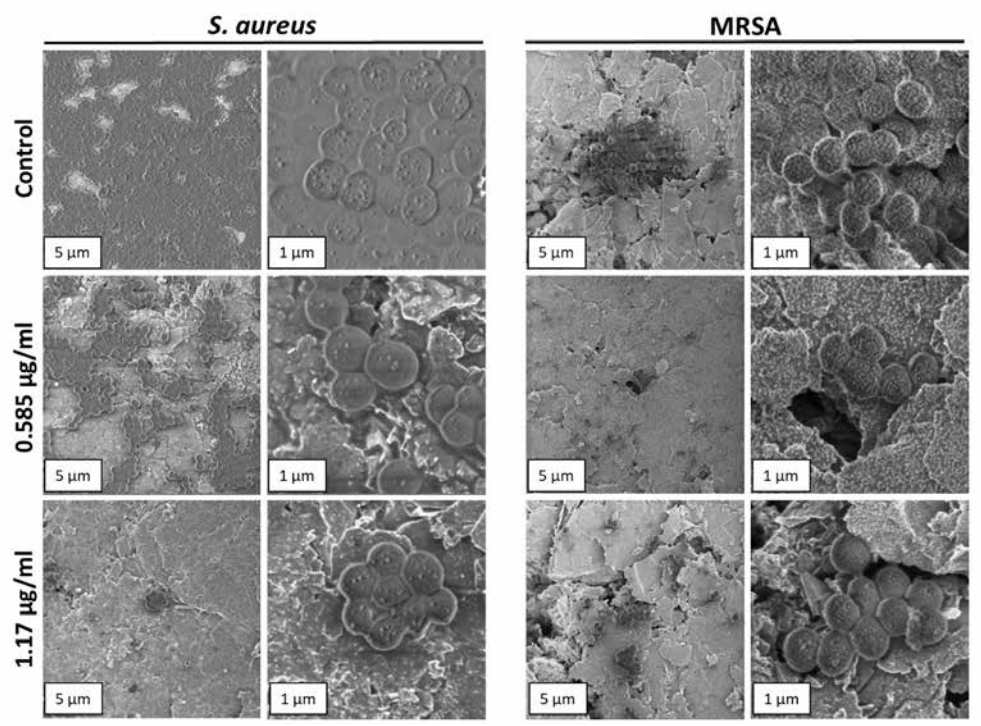

Fig. 4. Cryo-scanning electron microscopy images of the *Staphylococcus aureus* and methicillin-resistant *S. aureus* (MRSA) cells treated with poly(lactictide-co-glycolide) nanoparticles loaded with mupirocin at a concentration of either 0.585 μg/ml or 1.17 μg/ml (the scale bars are 5 and 1 μm)

Cytotoxicity testing

The *in vitro* putative cytotoxic activity of free MUP, encapsulated MUP (PLGA/MUP NPs) and empty PLGA NPs against keratinocyte cell line HaCaT was quantified by the MTT assay. Dependence of the cell viability percentage on the sample concentration is presented in Fig. 5. Despite the very high variability of the viability measurements within each of the tested concentrations, a tendency of encapsulated MUP to be less toxic for keratinocytes in comparison with both free MUP and empty PLGA can be inferred. No cytotoxic effect of encapsulated MUP was observed at the concentrations of 1–4 µg/ml, and keratinocyte viability was above 90% even after treatment with PLGA/MUP NPs at the concentration of 16 µg/ml. On the other hand, both free MUP and empty PLGA decreased cell viability below 85% already at the concentration of 2 µg/ml. No IC50 values (the half-maximal inhibitory concentration) were reached in the tested concentration range of any tested sample.

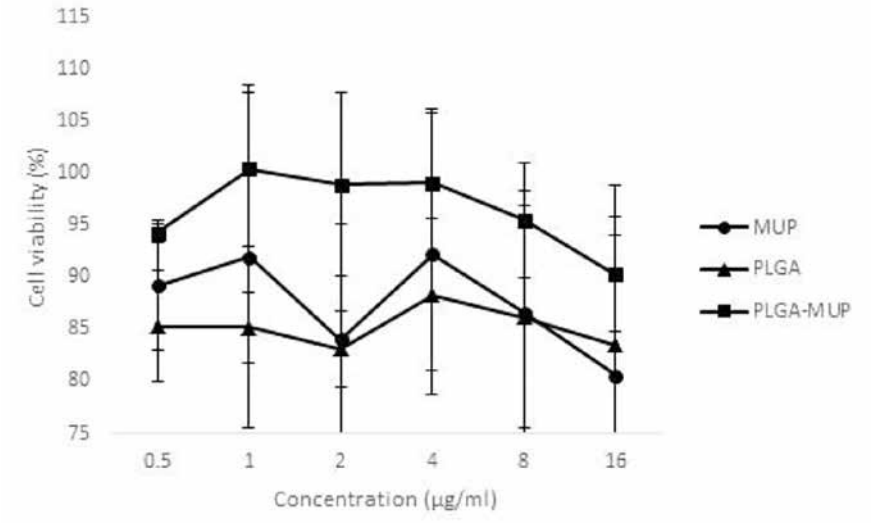

Fig. 5. Cytotoxic effects of empty poly(lactictide-co-glycolide) (PLGA) nanoparticles, poly(lactictide-co-glycolide) nanoparticles loaded with mupirocin (PLGA-MUP) and free mupirocin (MUP) on transformed aneuploid immortal keratinocyte cell line HaCaT analyzed by the dimethylthiazol-diphenyltetrazolium bromide (MTT) assay

Discussion

The main objective of the present experiment was to prove that antimicrobial effects of the antibiotic MUP entrapped in PLGA NPs are not inferior to free MUP, and at the same time that the composite PLGA/MUP NPs are fully biocompatible with skin cells, since these NPs are intended as an alternative auxiliary treatment of the cutaneous wounds. The reason for testing the alternatives is clear: the prevalence of heterogeneous MUP-resistant *S. aureus* strains is high (Mutu et al. 2022) and an efficient way to overcome the resistance is the application of NPs (Abo-Amer et al. 2022).

PLGA NPs used in the present study were already established as suitable carriers of drugs as far as tissue regeneration and wound healing is concerned (Arasoglu et al. 2016; He et al. 2018; Pourhojat et al. 2018; Naseri et al. 2020). However, regarding recent

experiments, the combination of PLGA/MUP was used rather scarcely: Naseri et al. (2020) introduced novel drug-eluting, bioabsorbable scaffold using MUP-loaded PLGA biomaterial ink including the 3D printing technique; the authors confirmed the efficacy of the biomaterial against *S. aureus*, similarly to the results of the present study.

When the disk diffusion method was applied in the present experiment, inhibitory effect of PLGA/MUP NPs at a concentration range from 0.29 to 1.17 μg/ml on *S. aureus* and MRSA did not differ from an effect of free MUP. Using the same method, Arasoglu et al. (2016) similarly reported a moderate antimicrobial activity of CAPE (caffeic acid phenethyl ester)/PLGA NPs against *S. aureus* and MRSA at concentrations of 30.63 and 61.25 μg/ml. Because the free CAPE did not have any antimicrobial activity, the results of the quoted study confirm, in agreement with the present experiment, a usefulness of the loaded PLGA NPs; according to the quoted authors (Arasoglu et al. 2016), antibacterial activity of the loaded PLGA NPs may be related to a higher penetration of active substances into the cells.

The relatively small areas of inhibition observed in the present experiment at higher concentrations of encapsulated MUP (1.17 and 2.34 μg/ml; Fig. 2) may be due to the insufficient ability of particles to penetrate through the culture media, because an overall antimicrobial effect is dependent solely on MUP released from the particles (Kourmouli et al. 2018). The concentrations shown in Fig. 2 are in μg/ml to be consistent with the data presented in other figures; the concentration of e.g. 2.34 μg/ml corresponds (after conversion) to 23.4 ng of MUP per disc. For the evaluation of the growth of *S. aureus* and MRSA, discs with penicillin and vancomycin, respectively, were used as the positive control for the following reason: the commercial MUP discs contain multiple times higher MUP concentrations compared to the PLGA-loaded MUP; for a proper comparison of inhibition zones, the same concentrations of antibiotics were applied in the discs as were those of MUP loaded in the nanoparticles.

Unloaded PLGA NPs did not affect growth curves of *S. aureus* or MRSA in the present study: no antimicrobial effect was expected as these NPs serve only as a carrier for a loaded drug (Kemme et al. 2018).

No apparent morphological changes in *S. aureus* and MRSA were observed in the present study using cryo-SEM technique (Fig. 4), but PLGA/MUP NPs, despite their negative ζ-potential, still showed antimicrobial activity against both tested bacteria. Similarly, Hasan et al. (2019) reported a significant decrease (2 log reduction) of MRSA viability using not only positively charged clindamycin-loaded PLGA NPs, but also their negatively charged counterparts. Because an attachment of negatively charged NPs to the surface of bacteria is feasible due to (among others) the electrostatic interaction (Hasan et al. 2019), the antibiotic activity of the composite particles in the present experiment can be explained by an uptake of the nano-encapsulated MUP and/or the controlled release of the drug over time.

According to ISO 10993-5 recommendations, cell viability higher than 70% analyzed by MTT indicates no cytotoxicity for the tested material (International Organization for Standardization 2009). This criterion has been met in the present experiment for both empty and loaded PLGA NPs, including free MUP, even at the concentration of 16 μg/ml.

Nevertheless, the biocompatibility of nano-encapsulated MUP still tended to be the highest in all tested samples (Fig. 5). The excellent biocompatibility of PLGA/MUP NPs with human keratinocyte cell line found in the present study agrees with the results of He et al. (2018) who reported an ideal biocompatibility with good cell adhesion of the antimicrobial peptide (Pac-525)-loaded PLGA microspheres using rat bone marrow mesenchymal stem cells. The results of He et al. (2018) and the present study also agree on the potential of both drug-loaded PLGA particles to inhibit bacterial (*S. aureus*) infection. Very similar conclusions regarding PLGA-based composite scaffolds as antimicrobial coverage for wounds with gram-positive bacteria were reported by Pourhojat et al. (2018),

who tested antibacterial property and biocompatibility (using the same method as applied in the present experiment: methyl-thiazolyl-tetrazolium assay) of PLGA nanofibres containing *Hypericum perforatum*. Cheng et al. (2021) reported a maximum tolerance concentration of 5 μg/ml for levofloxacin-loaded PLGA NPs to corneal epithelial cells. The authors argued that using PLGA NPs as a drug delivery system may decrease toxicity effects of the drug due to its slow release over time. Similarly, Hasan et al. (2019) found no significant cytotoxicity (> 93% viability) of clindamycin-loaded PLGA NPs to mouse fibroblasts.

On the other hand, no cytotoxic effect of empty PLGA nanoparticles was expected in the present study, so it is interesting that (though the differences were non-significant) empty PLGA NPs tended to decrease cell viability compared to PLGA-MUP NPs (Fig. 5). PLGA is a biodegradable polymer that has been approved by the European Medicines Agency and the US Food and Drug Administration as an ideal material for a drug delivery system due to its biocompatibility and biodegradability (Chiu et al. 2021); composite materials based on the PLGA NPs generally do not exhibit cytotoxic effects against eukaryotic cells (Burmistrov et al. 2022). Nevertheless, reduced viability of eukaryotic cells due to empty PLGA NPs has also been reported, including a possible explanation by their relatively slow biodegradation (Van de Ven et al. 2011).

It can be concluded that the nano-encapsulated MUP showed adequate antibacterial activity against *S. aureus* and MRSA strains, which was comparable with the effect of free MUP in the present experiment. Moreover, excellent biocompatibility of PLGA/MUP NPs was confirmed. The fact that PLGA/MUP NPs offer a promising strategy as part of the treatment of the healing of cutaneous wound has already been confirmed in our *in vivo* experiment using a porcine model (Komprda et al. 2022b).

Acknowledgements

This work was supported by the Internal Grant Agency of the Faculty of AgriSciences of the Mendel University in Brno (Project No. AF-IGA2019-TP006) and by the ERDF "Multidisciplinary research to increase application potential of nano-materials in agricultural practice" (Project No. CZ.02.1.01/0.0/0.0/16 025/0007314). The authors also thank Dr. Pavel Svec (Mendel University in Brno) for providing the Cryo-SEM analysis and Dr. Kristyna Smerkova and doc. Sona Hermanova (Mendel University in Brno) for manuscript editing.

References

Abo-Amer AE, Gad el-Rab SMF, Halawani EM, Niaz AM, Bamaga MS 2022: Prevalence and molecular characterization of methicilin-resistant *Staphylococcus aureus* from nasal specimens: Overcoming MRSA with silver nanoparticles and their applications. J Microbiol Biotechnol **32**: 1-10

Alcantara KP, Zulfakar MH, Castillo AL 2019: Development, characterization and pharmacokinetics of mupirocin-loaded nanostructured lipid carriers (NLCs) for intravascular administration. Int J Pharm **571**: 118705

Arasoglu T, Derman S, Mansuroglu B 2016: Comparative evaluation of antibacterial aktivity of caffeic acid phenethyl ester and PLGA nanoparticles formulation by different methods. Nanotechnology **27**: 025103

Astete CE, Sabliov CM 2006: Synthesis and characterization of PLGA nanoparticles. J Biomater Sci–Polym Ed **17**: 247-289

Basaran DDA, Gunduz U, Tezcaner A, Keskin D 2021: Topical delivery of heparin from PLGA nanoparticles entrapped in nanofibers of sericin/gelatin scaffolds for wound healing. Int J Pharm **597**: 120207

Berthet M, Gauthier Y, Lacroix C, Verrier B, Monge C 2017: Nanoparticle-based dressing: The future of wound treatment? Trends Biotechnol **35**: 770-784

Burmistrov DE, Simakin AV, Smirnova VV, Uvarov OV, Ivashkin PI, Kucherov RN, Ivanov VE, Bruskov VI, Sevostyanov MA, Baikin AS, Kozlov VA, Rebezov MB, Semenova AA, Lisitsyn AB, Vedunova MV, Gudkov SV 2022: Bacteriostatic and cytotoxic properties of composite material based on ZnO nanoparticles in PLGA obtained by low temperature method. Polymers **14**: 49

Cheng YH, Chang YF, Ko YC, Liu CJL 2021: Development of a dual delivery of levofloxacin and prednisolone acetate via PLGA nanoparticles/thermosensitive chitosan-based hydrogel for postoperative management: An *in-vitro* and *ex-vivo* study. Int J Biol Macromol **180**: 365-374

Chereddy KK, Her CH, Comune M, Moia C, Lopes A, Porporato PE, Vanacker J, Lam MC, Steinstraesser L, Sonveaux P, Huijun Z, Lino SF, Vandermeulen G, Préat V 2014: PLGA nanoparticles loaded with host defense peptide LL37 promote wound healing. J Control Release **194**: 138-147

Chiu HI, Samad NA, Fang L, Lim V 2021: Cytotoxicity of targeted PLGA nanoparticles: a systematic review. RCS Advances **11**: 9433-9449

Goldmann O, Cern A, Musken M, Rohde M, Weiss W, Barenholz Y, Medina E 2019: Liposomal mupirocin holds promise for systemic treatment of invasive *Staphylococcus aureus* infections. J Control Release **316**: 292-301

Hajipour MJ, Fromm KM, Ashkarran AA, de Aberasturi DJ, de Larramendi, IR, Rojo T, Serpooshan V, Parak WJ, Mahmoudi M 2012: Antibacterial properties of nanoparticles. Trends Biotechnol **30**: 499-511

Hasan N, Cao J, Lee J, Hlaing SP, Oshi MA, Naeem M, Ki MH, Lee BL, Jung Y, Yoo JW 2019: Bacteria-targeted clindamycin loaded polymeric nanoparticles: Effect of surface charge on nanoparticle adhesion to MRSA, antibacterial activity, and wound healing. Pharmaceutics **11**: 11050236

He YZ, Jin YH, Wang XM, Yao SL, Li YY, Wu Q, Ma GW, Cui FZ, Liu HY 2018: An antimicrobial peptide-loaded gelatin/chitosan nanofibrous membrane fabricated by sequential layer-by-layer electrospinning and electrospraying techniques. Nanomaterials **8**: 327

International Organization for Standardization, ISO 10993-5. Biological evaluation of medical services, Part 5: Tests for *in vitro* cytotoxicity. Geneva, Switzerland 2009.

Kemme M, Heinzel-Wieland R 2018: Quantitative assessment of antimicrobial activity of PLGA films loaded with 4-hexylresorcinol. J Funct Biomater **9**: 9010004

Khoshnood S, Heidary M, Asadi A, Soleimani S, Motahar M, Savari M, Saki M, Abdi M 2019: A review on mechanism of action, resistance, synergism, and clinical implications of mupirocin against *Staphylococcus aureus*. Biomed Pharmacother **109**: 1809-1818

Komprda T, Popelková V, Košarišťanová L, Šmídová V 2022a: Poly(lactic-co-glycolic) acid nanoparticles as a delivery system for fish oil in wound healing. Acta Vet Brno **91**: 285-291

Komprda T, Sládek Z, Vícenová M, Simonová J, Franke G, Kacvinská K, Sabliov S, Astete CE, Levá L, Popelková V, Bátik A, Vojtová L 2022b: Effect of polymeric nanoparticles with entrapped fish oil or mupirocin on skin wound healing using a porcine model. Int J Mol Sci **23**: 7663

Kourmouli A, Valenti M, van Rijn E, Beaumont HJE, Kalantzi OI, Schmidt-Ott A, Biskos G 2018: Can disc diffusion susceptibility tests assess the antimicrobial activity of engineered nanoparticles? J Nanopart Res **20**: 62

Lin YH, Lin JH, Hong YS 2017: Development of chitosan/poly-gamma-glutamic acid/pluronic/curcumin nanoparticles in chitosan dressings for wound regeneration. J Biomed Mater Res B **105**: 81-90

Ma P, Mumper RJ 2013: Anthracycline nano-delivery systems to overcome multiple drug resistance: A comprehensive review. Nano Today **8**: 313-331

Mutu E, Chen G, Liu R, Wang Y 2022: High prevalence of heterogeneous mupirocin-resistent *Staphylococcus aureus* and its molecular characterization. Am J Translat Res **14**: 8243-8251

Naseri E, Cartmell C, Saab M, Kerr RG, Ahmadi A 2020: Development of 3D printed drug-eluting scaffolds for preventing piercing infection. Pharmaceutics **12**: 901

Perumal PG, Kannan S, Appalaraju B 2022: Detection and distribution of low level and high level mupirocin resistance among clinical methicillin resistant *Staphylococcus aureus* isolates. J Clin Diagnos Res **16**: DC06-DC10

Pourhojat F, Shariati S, Sohrabi M, Mahdavi H, Asadpour L 2018: Preparation of antibacterial electrospun polylactic-co-glycolic acid nanofibers containing *Hypericum perforatum* with bedsore healing property and evaluation of tis drug release performance. Int J Nano Dimens **9**: 286-297

Rajendran NK, Kumar SSD, Houreld NN, Abrahamse H 2018: A review on nanoparticle based treatment for wound healing. J Drug Deliv Sci Technol **44**: 421-430

Smith R, Russo J, Fiegel J, Brogden N 2020: Antibiotic delivery strategies to treat skin infections when innate antimicrobial defense fails. Antibiotics-Basel **9**: 9020056

Sundaramoorthy M, Karuppaiah A, Nithyanth M, Baberoselin R, Ramesh S, Geetha N, Veintramuthu S 2021: Formulation development of cream with mupirocin and essential oils for eradication of biofilm mediated antimicrobial resistance. Arch Microbiol **203**: 1707-1715

Tang ZY, Ma QT, Chen XL, Chen TB, Ying Y, Xi XP, Wang L, Ma CB, Shaw C, Zhou M 2021: Recent advances and challenges in nanodelivery systems for antimicrobial peptides (AMPs). Antibiotics-Basel **10**: 10080990

Van de Ven H, Vermeersch M, Matheeussen A, Vandervoort J, Weyenberg W, Apers S, Cos P, Maes L, Ludwig A 2011: PLGA nanoparticles loaded with the antileishmanial saponin β-aescin: Factor influence study and *in vitro* efficacy evaluation. Int J Pharm **420**: 122-132

Vymazalova P, Popelkova V, Komprda T, Sabliov C, Astete CE 2020: Synthesis of PLGA nanoparticles with entrapped antibiotic mupirocin. Proc Int PhD Stud Conf Mendel Net pp. 589-593

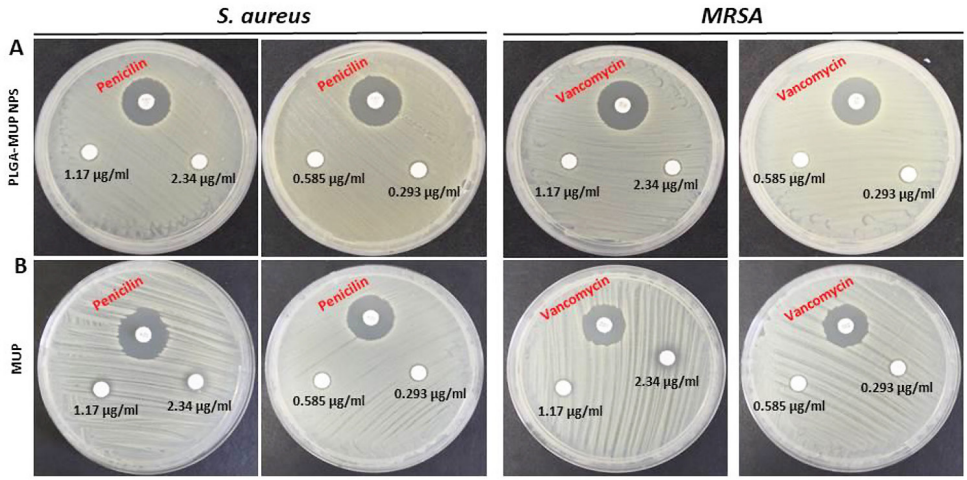

Fig. 2. The width of an inhibition zone surrounding a cellulose disc (6 mm diameter) impregnated with different concentrations of poly(lactictide-co-glycolide) nanoparticles loaded with mupirocin (PLGA-MUP; A) or free mupirocin (MUP; B) in presence of *Staphylococcus aureus* and methicillin-resistant *S. aureus* (MRSA); penicillin and vancomycin were used as a positive control

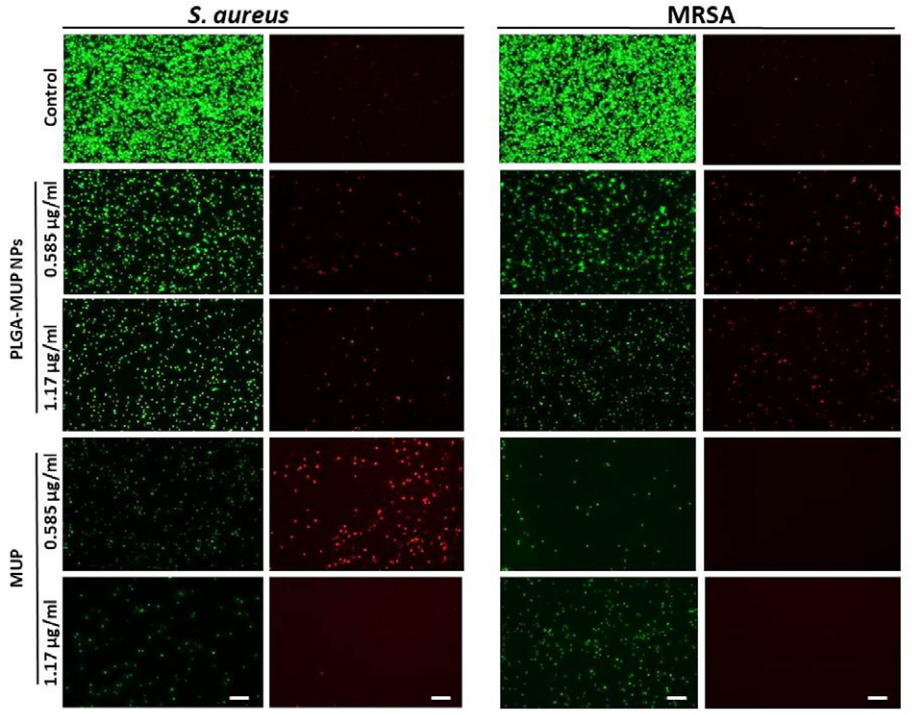

Fig. 3. Fluorescence microscopy of live + dead cells (green spots) and dead cells (red spots) of *Staphylococcus aureus* and methicillin-resistant *S. aureus* (MRSA) strains treated with poly(lactictide-co-glycolide) nanoparticles loaded with mupirocin (PLGA-MUP) or free MUP, at MUP concentration of either 0.585 µg/ml or 1.17 µg/ml (the scale bar is 20 µm; the brightness and contrast were processed equally across all micrographs)